Pullout Behaviour of Steel Under Different Types of Concrete Composites

Sunil C. Behanan*, Dr. Bindhu K. R., Adithya D. A.

Department of Civil Engineering, College of Engineering Trivandrum, Affiliated to APJ Abdul Kalam Technological University, Kerala, India

*Corresponding author's e-mail: sunilbehanan@gmail.com

doi: https://doi.org/10.21467/proceedings.156.3

ABSTRACT

In reinforced-concrete members adequate bond strength between reinforcing bars is necessary to guarantee full composite action. The present study involves the analysis of bond strength by conducting pullout test on deformed steel rebar embedded in various types of concrete such as normal concrete, engineered cementitious composite (ECC) and glass powder concrete (GPC). ECC has ductility due to presence of fibre which prevents development of internal cracks, and it has more compatible deformability with steel rebar. The bond between concrete and steel is not uniform and differ with different loading condition. Other factors like mechanical interlocking, adhesion between concrete and steel also contribute to bond. Earthquake forces causes reversal of load and hence at lap joints it can cause slip of the joints if sufficient anchorage length is not given. Pullout studies were conducted to assess the bond characteristics of concrete and steel using cube and cylindrical specimens as per the current standards/codes. The bond slip behavior acquired from the pullout test using the software "ANSYS" were equated with the experimental results. The bond strength of ECC and GPC are more compared to that of M30 using same strength of concrete composites. All load-slip curves have mostly the same trend for M30, GPC and ECC. Comparison of numerical results with experimental results gave less than 6% error for concrete composites. From both experimental and numerical studies, failure is more critical at the interface region of concrete composites and steel bar.

Keywords: Pullout, Concrete composites, Modeling

1 Introduction

The bond between concrete and steel is not uniform and differ with different loading condition [1]–[4]. Earthquake forces causes reversal of load and hence at lap joints it can cause slip of the joints if sufficient anchorage length is not given [5]–[8]. The present study involves the investigation of bond strength by conducting pull-out test on deformed steel rebar embedded in various types of concrete such as normal concrete, engineered cementitious composite (ECC) and glass powder concrete (GPC) [9].

Engineered Cementitious Composites (ECC) consists primarily of fibers, fine aggregates, cement [10]. In uniaxial tension it has better strain hardening behaviour and ultra-high strain capacity in contrast to normal concrete [11]–[13]. ECC has been applied in structural elements because of its extraordinary mechanical properties, mainly in shear and flexural-dominated members, such as low-rise walls, coupling beams and beam-column joints [14], [15].

2 Materials and Methods

The experiment was designed to find out about the bond behaviour such as bond strength, failure pattern, load-slip curve and failure mode of concrete composites such as conventional concrete, glass powder concrete and ECC.

2.1 Arriving mix proportion of materials

The material properties are displayed in table 1:

Proceedings DOI: 10.21467/proceedings.156; Series: AIJR Proceedings; ISSN: 2582-3922; ISBN: 978-81-961472-7-3

Table 1: *Material Properties*

Cement	53 Grade OPC
Specific gravity of cement	3.15
Specific gravity of coarse aggregate	2.768
Specific gravity of fine aggregate	2.58
Density of glass powder	2300 kg/mm^3
Density of cement	2300 kg/mm^3
Density of fly ash	1378 kg/mm^3

The concrete properties are displayed in table 2:

Table 2: *Concrete Properties*

CONCRETE TYPE	M30	ECC	GPC
Young's Modulus	26187 MPa	22200 MPa	34562 MPa
Poisson's ratio	0.15	0.16	0.2
Water cement ratio	0.48	0.5	0.48
Mix Proportion	Cement : Fine Aggregate : Coarse Aggregate= 1 : 1.795: 3.01	Cement : Fine Aggregate : Fly ash : Steel fibre : PVA = 1 : 1.2 : 0.4 : 1.5 : 0.5	Cement : Glass powder : Fine Aggregate: Coarse Aggregate= 1 : 0.25 :2.244 : 3.76
Compressive Strength	37.8 MPa	38 MPa	38 MPa

2.2 Casting of specimens

Three different concrete mixes were prepared. Deformed reinforcing bars having nominal diameter of 16 mm shown in Fig. 2 was inserted in each of the concrete mixes. Cube of size 150x150x150 mm for conventional concrete, glass powder concrete and ECC were cast. That is total three specimens. Spring/Helix of 6 mm diameter and 25 mm pitch was inserted for confinement as per IS 2770 (Part-1) is shown in Fig. 1 and Fig. 3. The cross-section of the square specimens for pull-out test is150 mm×150 mm and the embedment length of the bar is 150 mm. The steel rebar was inserted in the centre of concrete specimen such that 840 mm of the rebar length is sticking out on one end and 10 mm of the rebar on the other end. This was done in order to obtain the measurements for rebar slip and for convenience of grip during pull-out tests. The pull-out test specimens were tested after 28 days of curing as shown in Fig. 4 after casting.

Figure 1: *Mould and helical spring*

Figure 2: *16mm diameter reinforcing bar and concrete mix.*

Figure 3: *Inserting helical spring and sample specimen after casting.*

Figure 4: *Curing of specimens.*

Proceedings DOI: 10.21467/proceedings.156
ISBN: 978-81-961472-7-3

Series: AIJR Proceedings
ISSN: 2582-3922

2.3 Experimental setup

The test setup consists of an assembly on which the pull-out specimen could be attached on the UTM (universal testing machine). The concrete cube was rested against the steel plate of the assembly such that the rebar could pass through the central hole as shown in Fig. 5.

Figure 5: *Test setup*

Figure 6: *LVDT and strain gauge*

Figure 7: *T-SCOPE (Data acquisition system)*

This experimental setup literally provided the needed resistance against the loading thus forming the pull-out mechanism. LVDT (linear variable differential transformer) is used to measure the slip in the rebar. The LVDT is mounted on top of the free end of rebar as shown in Fig. 6. T-Scope (data acquisition system) is used to record the displacement from LVDT which is connected as shown in fig. 7 and the corresponding load was noted at regular interval of 50 kg load increment on UTM. Strain gauges of 5 mm length with 150 ohms was attached to the rebar at the region above the upper surface of the concrete cube.

3 Results and Discussion

3.1 Experimental Results

3.1.1 Result of M30 specimen

The load-slip relationship for M30 specimen tested is shown in Fig 8 and the breaking load observed was 724.1 N.

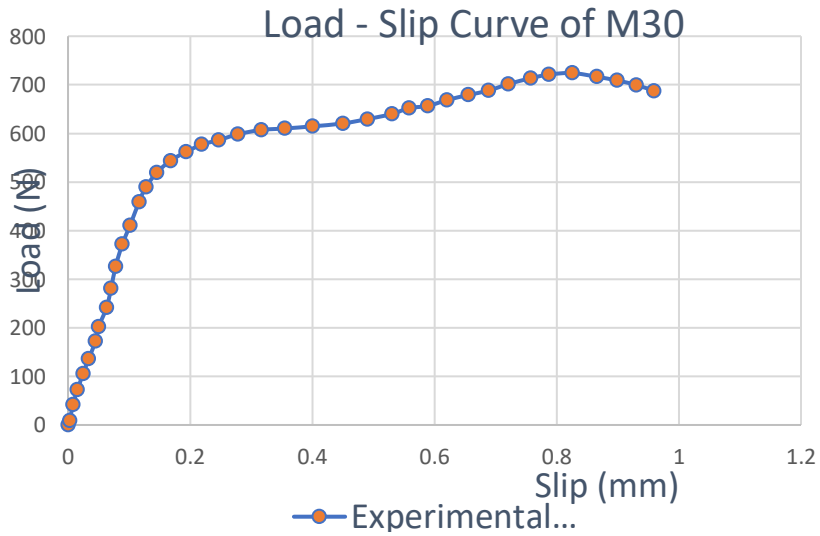

Figure 8: *Load-Slip Curve of M30*

Proceedings DOI: 10.21467/proceedings.156
ISBN: 978-81-961472-7-3

Series: AIJR Proceedings
ISSN: 2582-3922

With the formation of longitudinal cracks immediately the failure happens. When cracking occurs, the bond forces are outwardly directed from the bar surface which give rise to anchorage failure resulting in confining concrete splitting. The failure mode for a normal pull-out specimen for a 150 mm embedment length is shown in Fig.9.

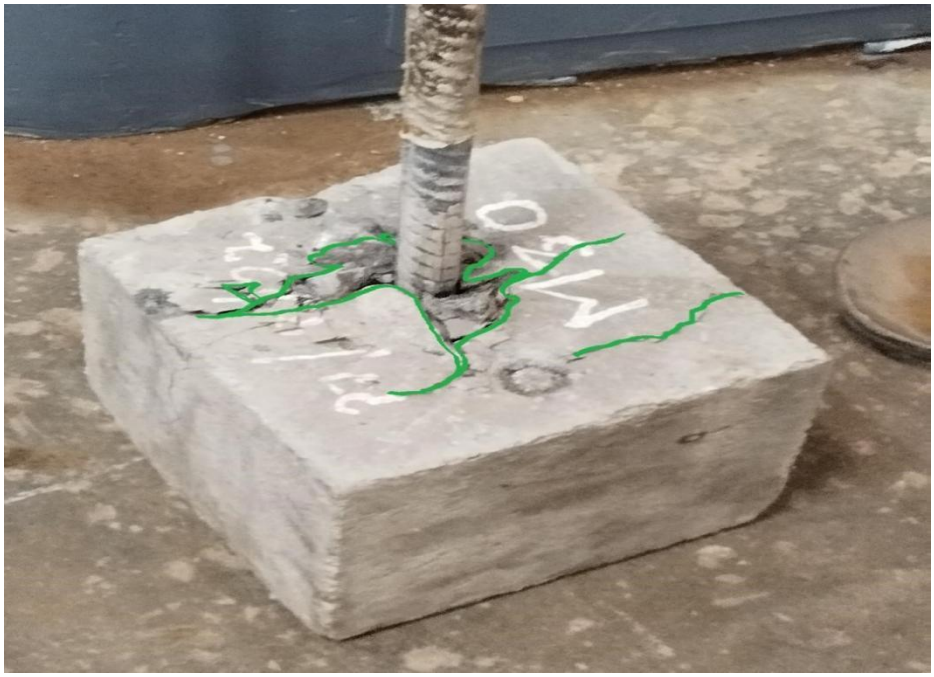

Figure 9: *Failure pattern of M30*

3.1.2 Results of GPC specimen

The load-slip relationship for GPC specimen tested is shown in Fig 10 and the breaking load observed was 881.9 N.

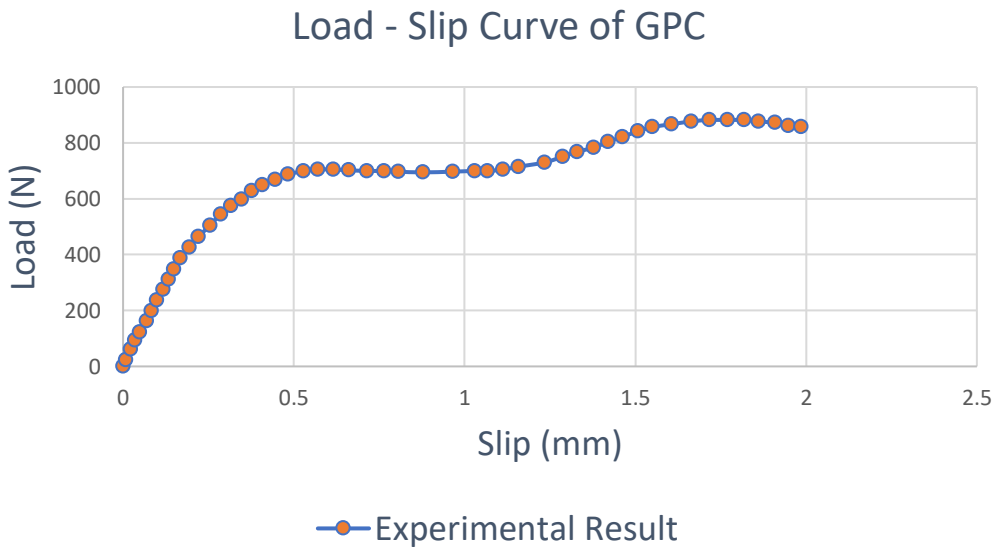

Figure 10: *Load-Slip Curve of GPC*

Cone failure occurred on the upper portion of concrete and also anchorage failure had occurred. Uncracked concrete portions are also present in the concrete specimen.

Figure 11: *Failure pattern of GPC*

3.1.3 Results of ECC specimen

The load-slip relationship for ECC specimen tested is shown in Fig. 12 and the breaking load observed was 899.5 N. The deformed steel rebar embedded in ECC as displayed in Fig. 12 and Fig. 13, the cracks started due to the phenomenon of stress concentration between ECC and steel ribs. However, during its extension each fissure turned to be micro cracks. This is credited to the bridge-effect of PVA and steel fibers in ECC matrix that could successfully control the expansion of cracks.

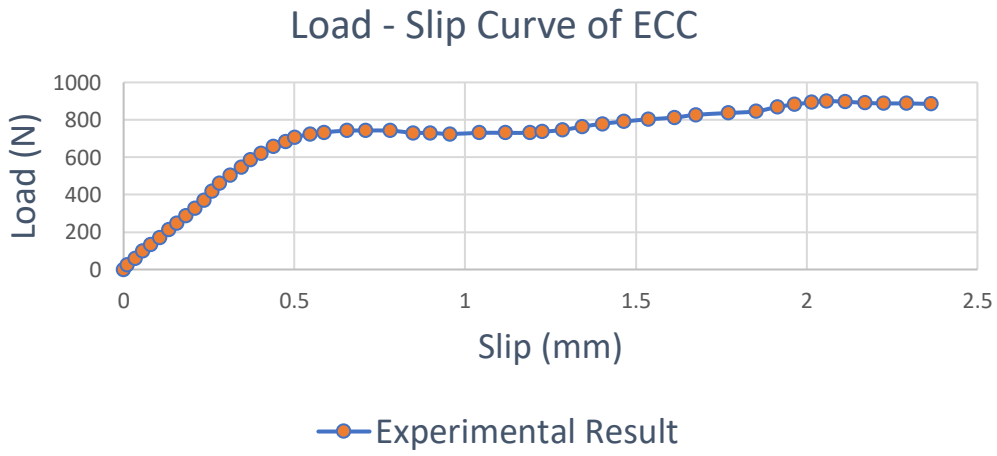

Figure 12: *Load- Slip Curve of ECC*

Proceedings DOI: 10.21467/proceedings.156
ISBN: 978-81-961472-7-3

Series: AIJR Proceedings
ISSN: 2582-3922

Figure 13: *Failure of ECC specimen*

Figure 14: *Failure pattern of ECC*

3.1.4 Comparison of results

From the comparison of load-slip curve, ECC and GPC specimens have more bond strength compared to M30 specimen which can be easily identified from Fig. 15.

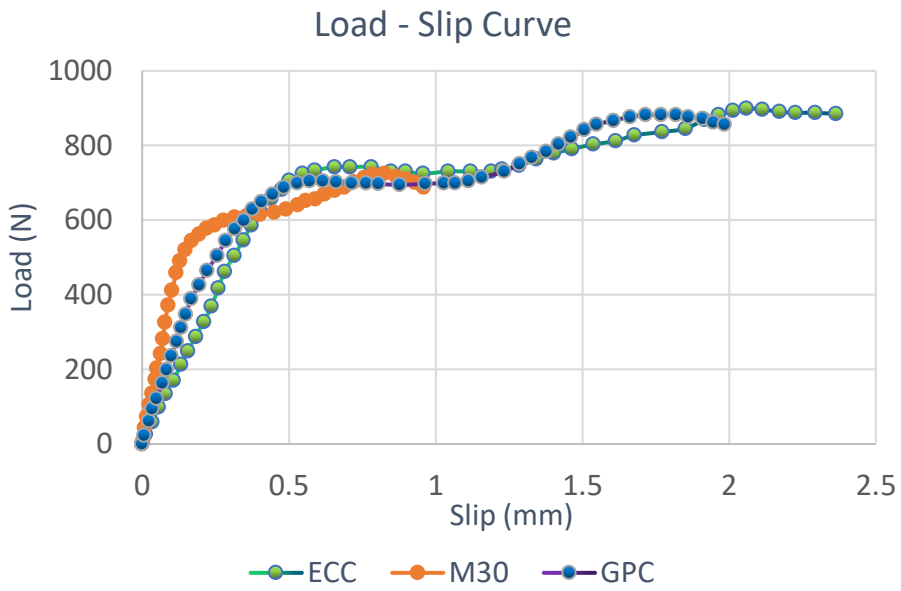

Figure 15: *Load-Slip Curve of experimental results*

3.2 Finite Element Modelling

3.2.1 Validation of numerical study with literature

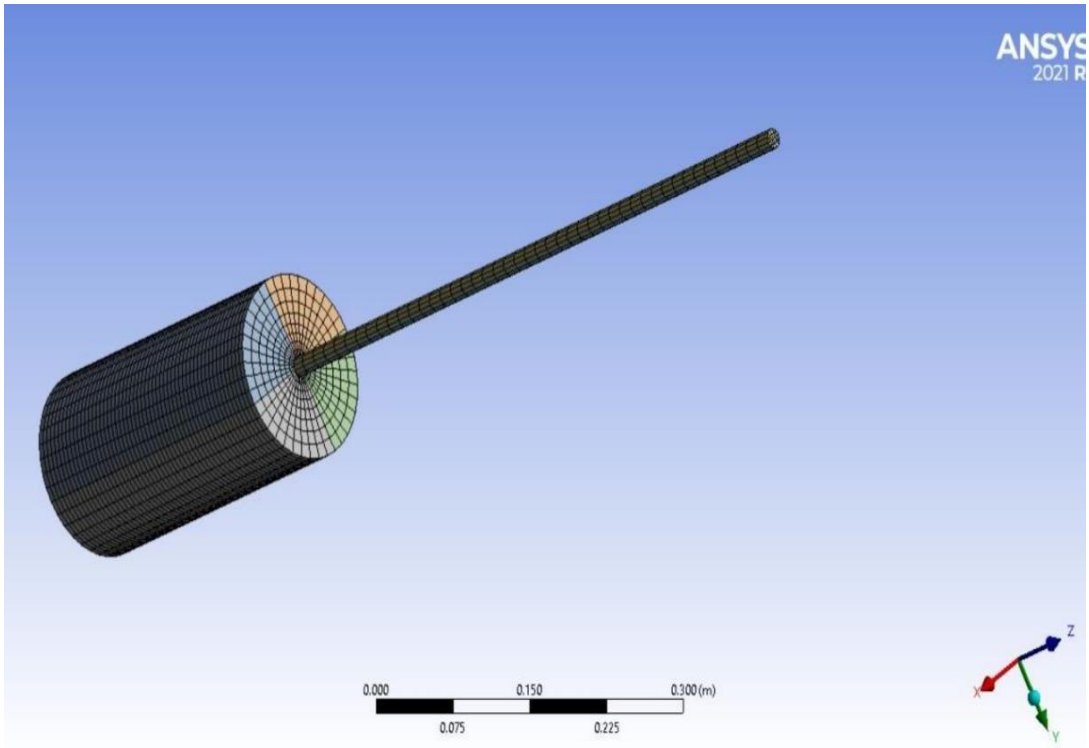

Figure 16: *Model of specimen used for validation*

Validation had done with the literature Al-Zuhairi and Al-Fatlawi, 2013 by finite element analysis with ANSYS software [16]. The model of the specimen used for validation is displayed in the Fig. 16.
Details of the modelled specimen is displayed in table 3.

Proceedings DOI: 10.21467/proceedings.156
ISBN: 978-81-961472-7-3

Series: AIJR Proceedings
ISSN: 2582-3922

Table 3: *Details of specimen validated.*

Dimension of cylinder	150 mm-diameter, 300 mm height
Bar dimension	16 mm diameter, 1 m length
Element order	Linear
Transition	Slow
Span angle center	Coarse
Initial size seed	Assembly
Bounding box diagonal	1.0223 m
Average surface area	8.9696e-003 m²
Minimum edge length	8.e-003 m
Quality of mesh	High

3.2.2 Results of Validation

Similar bond stress-slip curve obtained for the modelled specimen as displayed in Fig. 17.

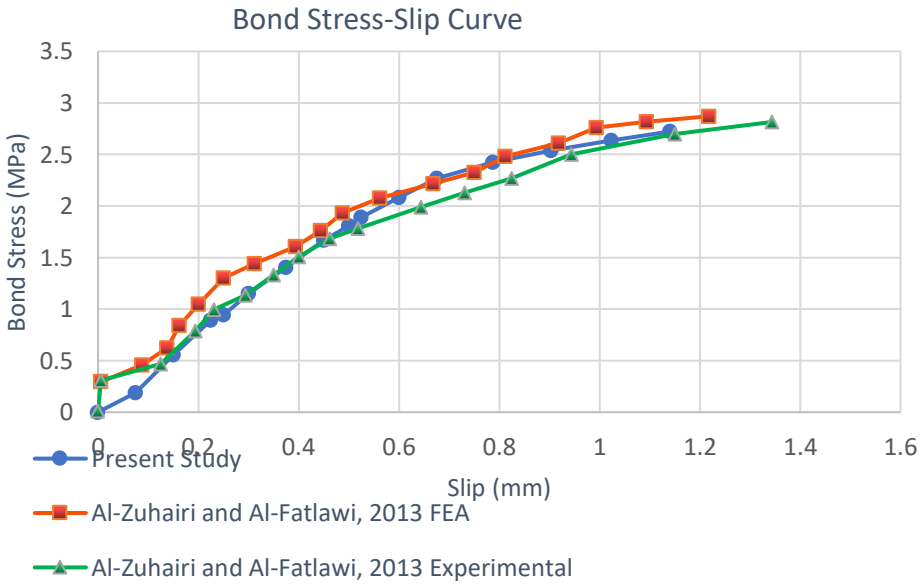

Figure 17: *Bond stress- Slip Curve*

The error occurred in the validation is 5.14 % and 3.092 % with respect to numerical and experiment results in the literature and which is shown in table 4.

Table 4: *Error occurred in validation*

	(Al-Zuhairiand Al-Fatlawi, 2013)- Experimental	(Al-Zuhairi and Al-Fatlawi, 2013)- Numerical	Present Experimental Study	Percentage error (FEA)	Percentage error (Experimental)
Average bond stress maximum (MPa)	2.81	2.870	2.723	5.140	3.092

3.3 Numerical Study

3.3.1 Modelling of Specimen

Specimen similar to those cast for the experimental study were modelled for numerical study. The numerical model of the specimen is displayed in Fig. 19 and the helical spring is displayed in Fig. 18. And specifics of the numerical model are given in table 5.

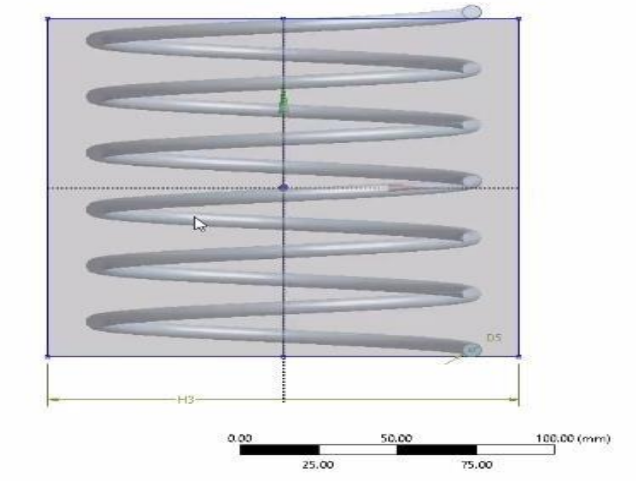

Figure 18: *Helical spring inside specimen*

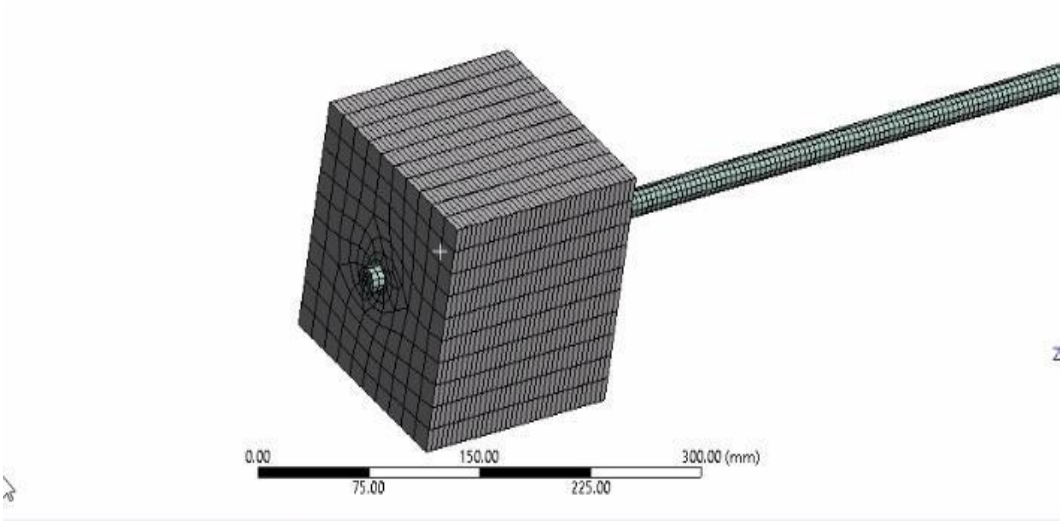

Figure 19: *Numerical model*

Table 5: *Details of numerical model*

Dimension of cube	150 mm X 150 mm X 150 mm
Bar dimension	16 mm diameter, 1 m length
Element order	Linear
Transition	Slow
Span angle center	Coarse

Proceedings DOI: 10.21467/proceedings.156
ISBN: 978-81-961472-7-3

Series: AIJR Proceedings
ISSN: 2582-3922

Initial size seed	Assembly
Bounding box diagonal	1.0223 m
Average surface area	8.9696e-003 m²
Minimum edge length	8.e-003 m
Quality of mesh	High

The numerical study was carried out in similar conditions of support and loading as done experimentally which is displayed in Fig. 20.

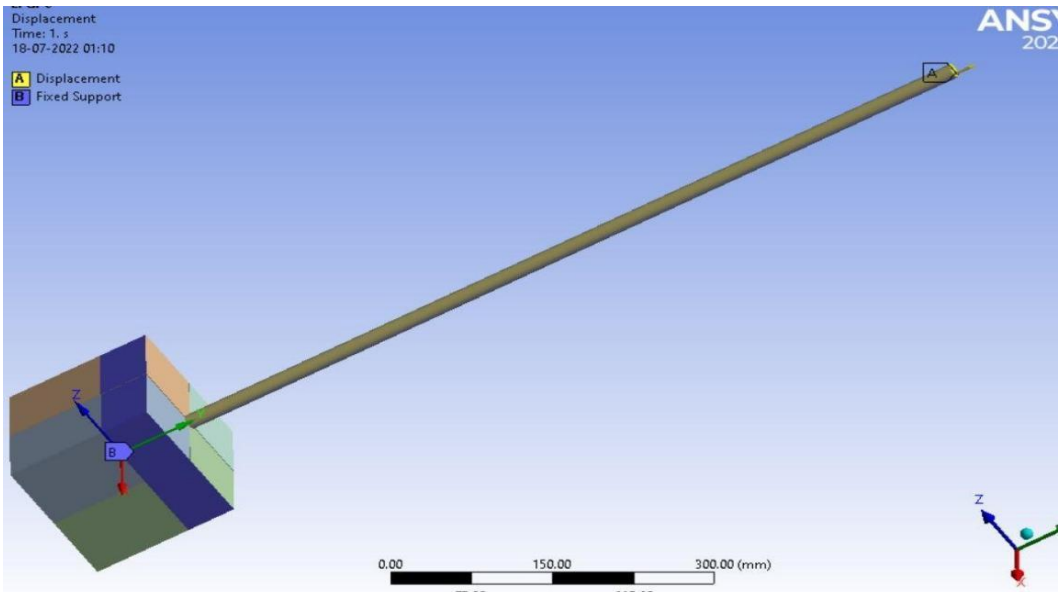

Figure 20: *Loading of specimen for numerical study.*

3.3.2 Results of M30 specimen

The load-slip curve of M30 specimen is displayed in Fig. 21 and the stress distribution is found maximum at the interface of rebar and concrete as displayed in Fig. 22.

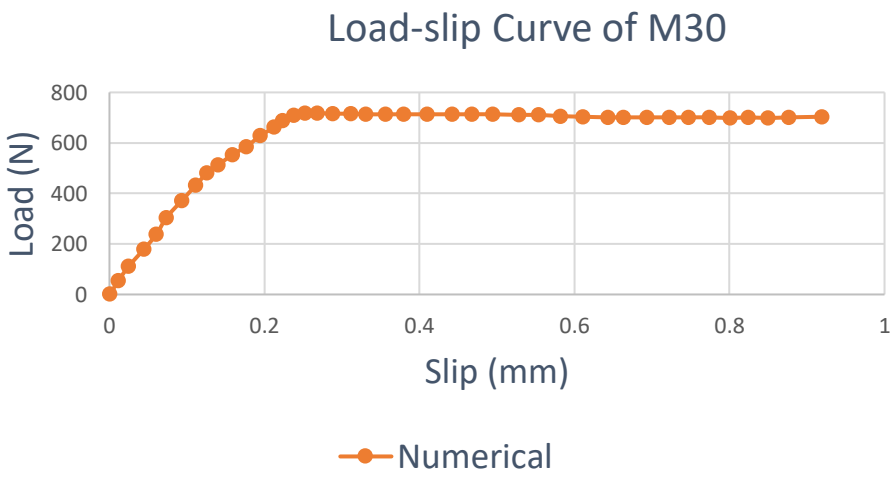

Figure 21: *Load-Slip curve of M30 specimen*

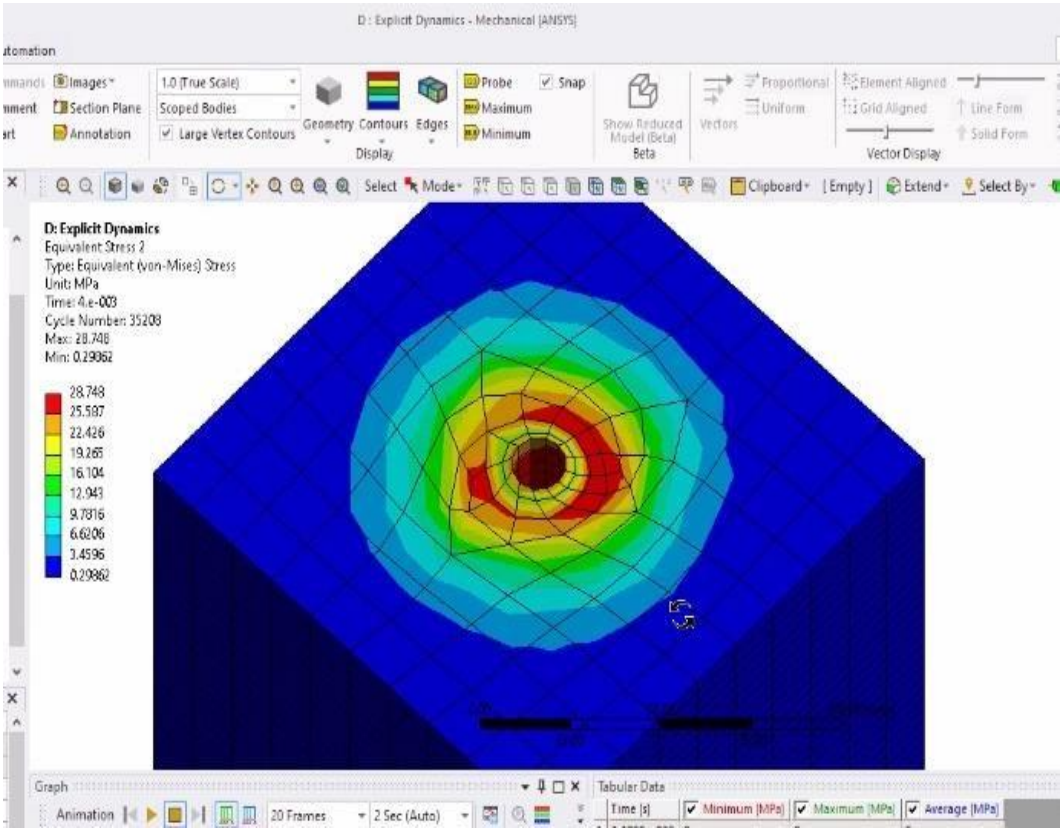

Figure 22: *Stress distribution in M30 specimen*

3.3.3 Results of GPC specimen

The load-slip curve of GPC specimen is displayed in Fig. 23 and the stress distribution is found maximum at the interface of rebar and concrete as displayed in Fig. 24.

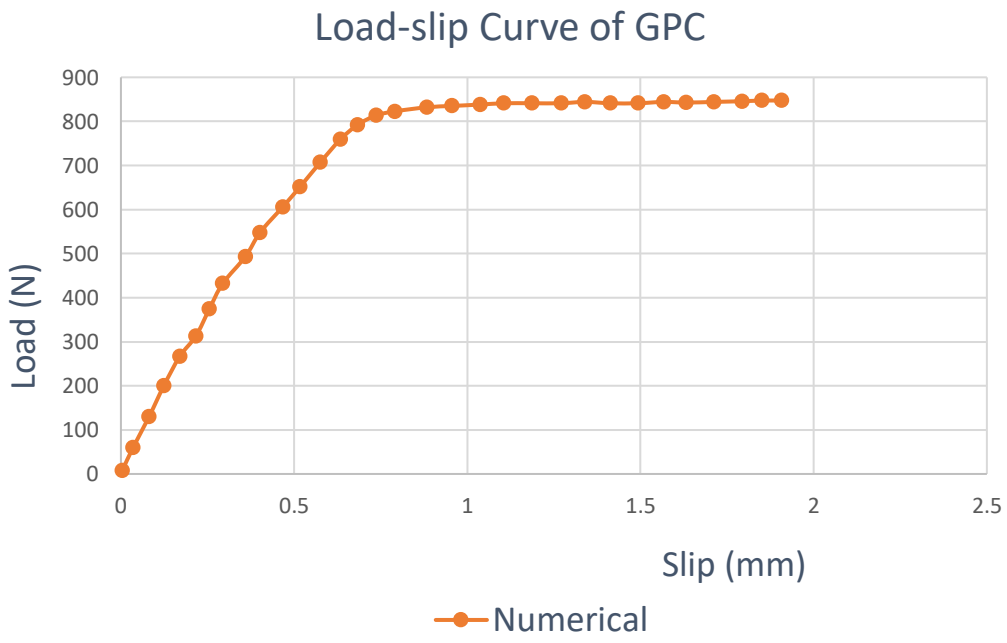

Figure 23: *Load-Slip Curve of GPC specimen*

Proceedings DOI: 10.21467/proceedings.156
ISBN: 978-81-961472-7-3

Series: AIJR Proceedings
ISSN: 2582-3922

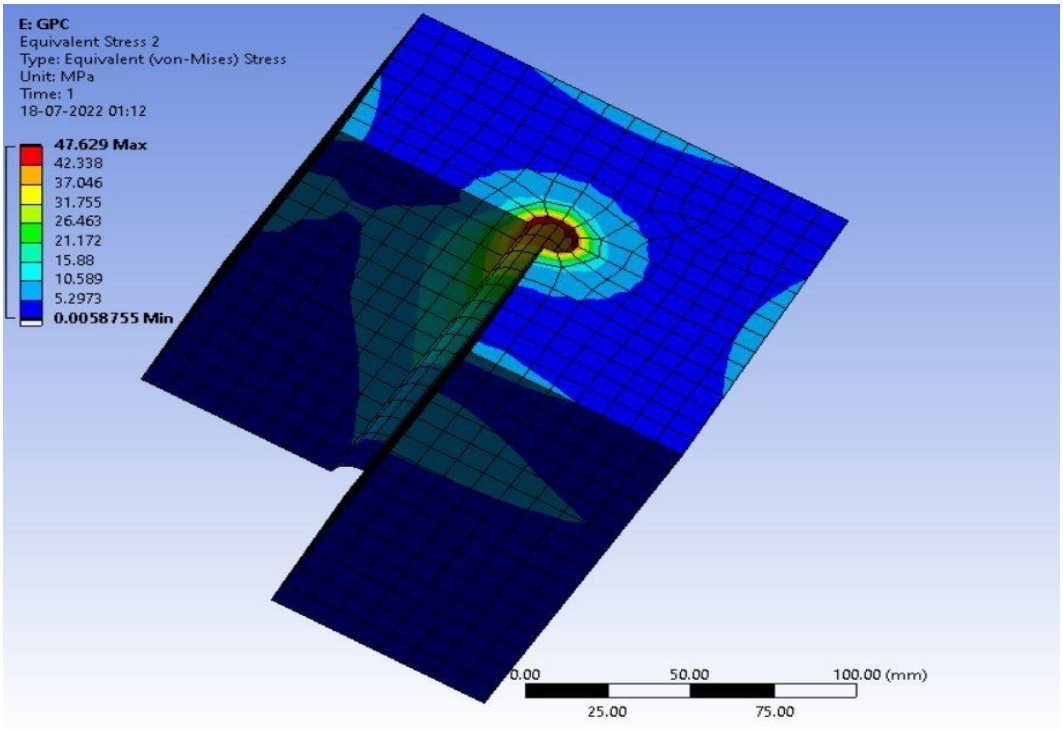

Figure 24: *Stress distribution in GPC specimen*

3.3.4 Results of ECC specimen

The load-slip curve of ECC specimen is displayed in Fig. 25 and the stress distribution is found maximum at the interface of rebar and concrete as displayed in Fig. 26.

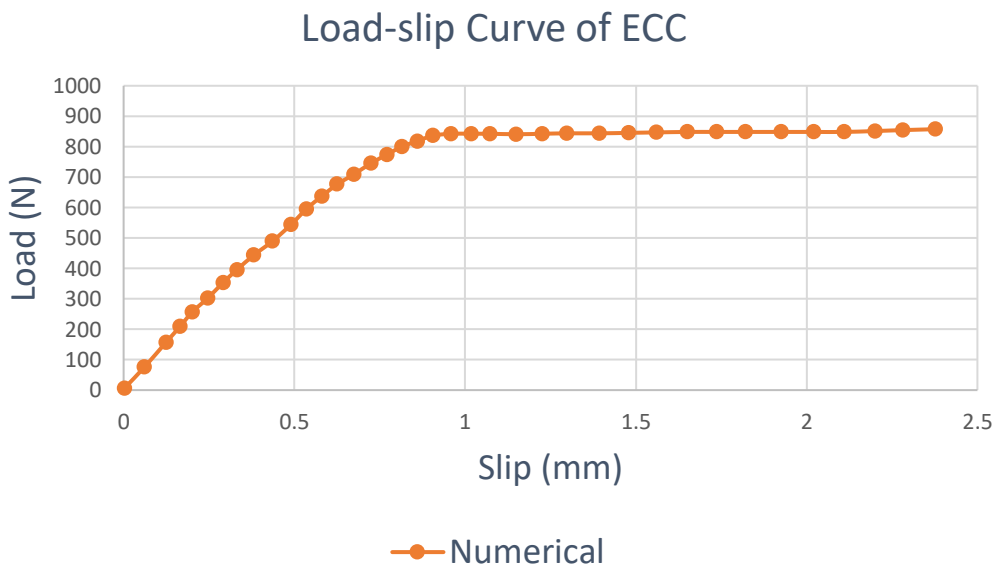

Figure 25: *Load-Slip Curve of ECC specimen*

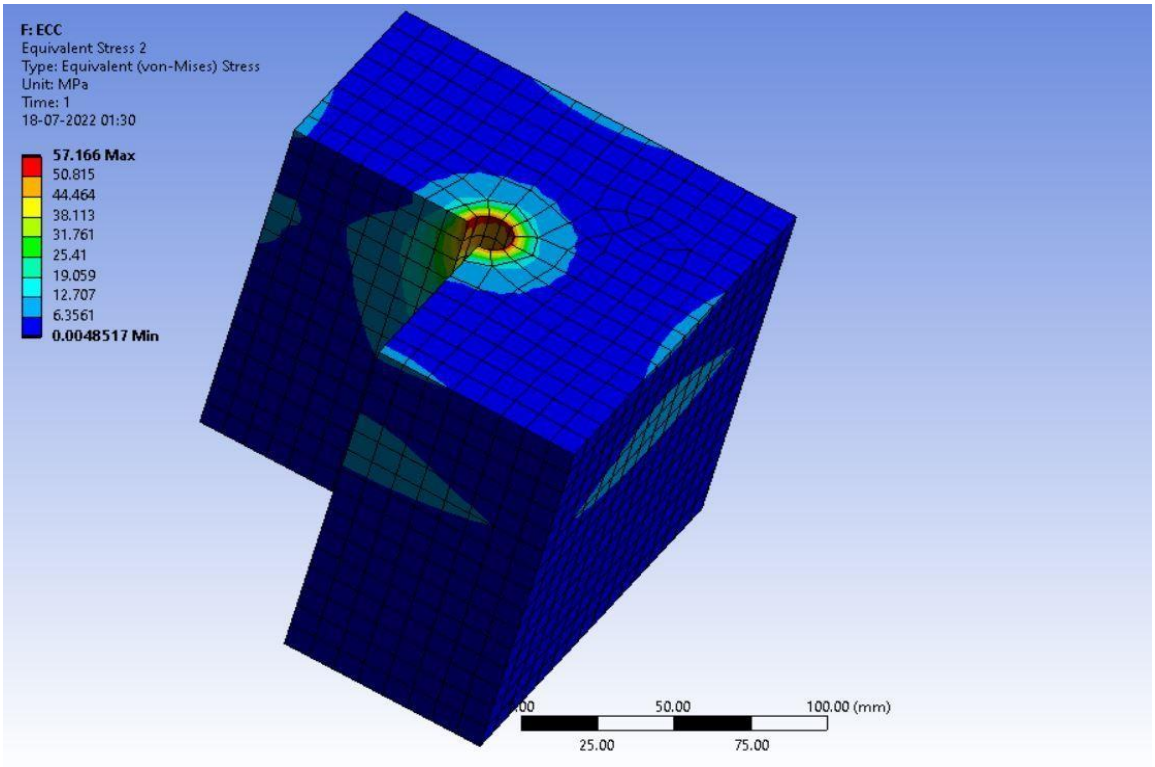

Figure 26: *Stress distribution in ECC specimen*

3.3.5 Comparison of numerical results

From the comparison of numerical results, ECC and GPC specimens have more bond strength compared to M30 specimen which can be easily identified from Fig. 27.

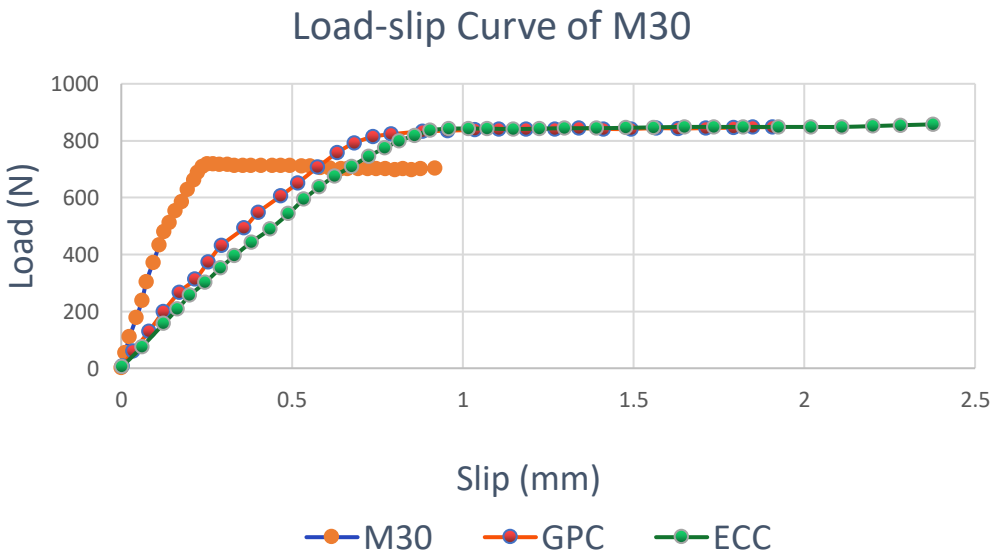

Figure 27: *Comparison of numerical results*

3.4 Comparison of numerical results with experimental results

3.4.1 M30 specimen

The comparison of numerical result with experimental result of load-slip curve of M30 specimen is shown in Fig. 28.

Proceedings DOI: 10.21467/proceedings.156
ISBN: 978-81-961472-7-3

Series: AIJR Proceedings
ISSN: 2582-3922

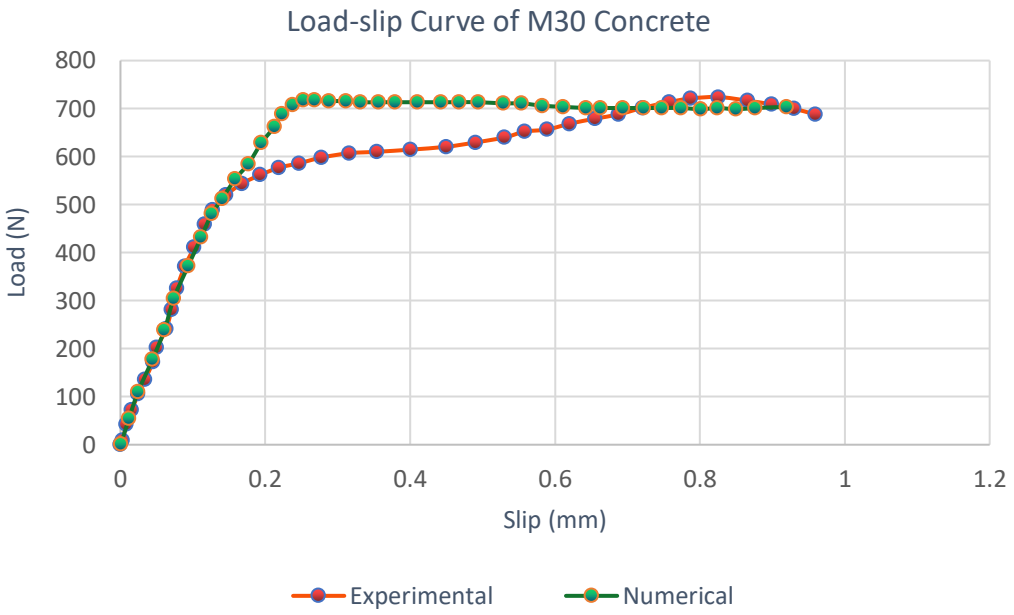

Figure 28: *Comparison of load-slip curve of M30*

3.4.2 GPC specimen

The comparison of numerical result with experimental result of load-slip curve of GPC specimen is shown in Fig. 29.

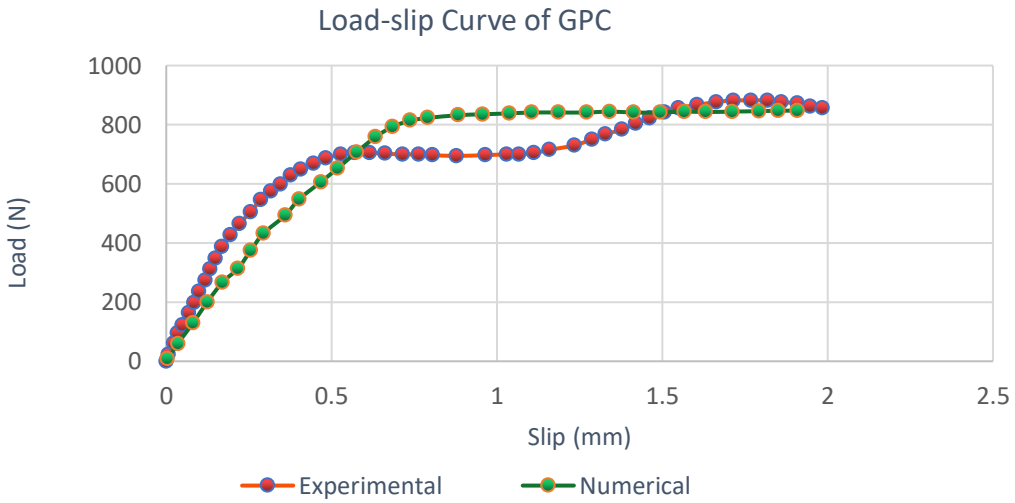

Figure 29: *Comparison of load-slip curve of GPC*

3.4.3 ECC specimen

The comparison of numerical result with experimental result of ECC specimen's load-slip curve is displayed in Fig. 30.

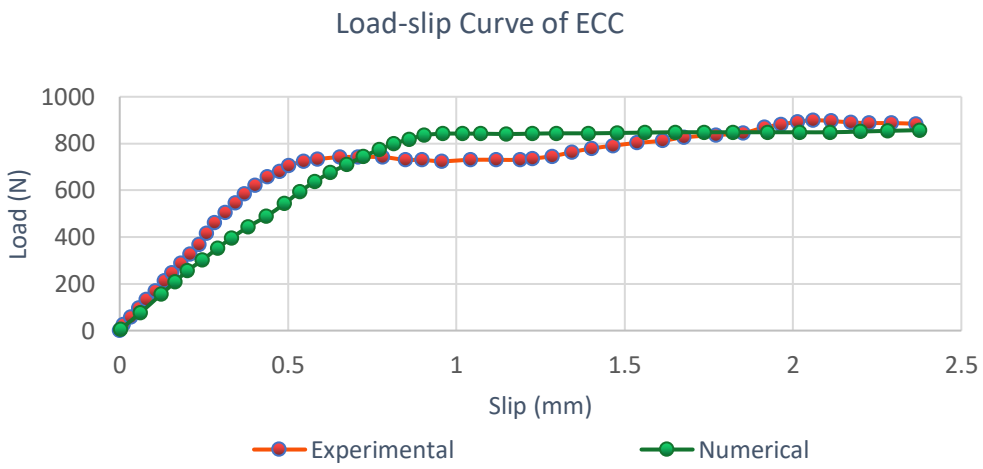

Figure 30: *Comparison of load-slip curve of ECC*

3.4.4 Comparison of Results

There is only small deviation of numerical results with that of experimental results of less than 6% as shown in table 6.

Table 6: *Comparison of numerical results with experimental results*

	Maximum Load (N) Numerical Result	Maximum Load (N) Experimental Result	Percentage error
M30	713.7	724.1	1.43
GPC	850.4	881.9	3.57
ECC	853.2	899.5	5.14

4 Conclusions

The bond strength of ECC and GPC are more compared to that of M30 using same strength of concrete composites. All load-slip curves have mostly the same trend for M30, GPC and ECC and only magnitude of the load carrying capacity with respect to slip had increased for ECC and GPC compared to M30. Comparison of numerical results with experimental results gave less than 6% error for concrete composites. That is the results obtained from numerical study matches well with the experimental results. From both experimental and numerical studies, failure is more critical at the interface region of concrete composites and steel bar.

5 Publisher's Note

AIJR remains neutral with regard to jurisdictional claims in institutional affiliations.

How to Cite

Behanan *et al.* (2023). Pullout Behaviour of Steel Under Different Types of Concrete Composites. *AIJR Proceedings*, 16-33. https://doi.org/10.21467/proceedings.156.3

References

[1] H. Huang, Y. Yuan, W. Zhang, R. Hao, and J. Zeng, "Bond properties between GFRP bars and hybrid fiber-reinforced concrete containing three types of artificial fibers," *Constr Build Mater*, vol. 250, Jul. 2020, doi: 10.1016/J.CONBUILDMAT.2020.118857.

[2] X. Li, Y. Bao, N. Xue, and G. Chen, "Bond strength of steel bars embedded in high-performance fiber-reinforced cementitious composite before and after exposure to elevated temperatures," *Fire Saf J*, vol. 92, pp. 98–106, Sep. 2017, doi: 10.1016/J.FIRESAF.2017.06.006.

[3] H. O. Shin, S. J. Lee, and D. Y. Yoo, "Bond Behavior of Pretensioned Strand Embedded in Ultra-High-Performance Fiber-Reinforced Concrete," *Int J Concr Struct Mater*, vol. 12, no. 34, pp. 1–13, Apr. 2018, doi: 10.1186/S40069-018-0249-4.

[4] J. Zhang, F. Bian, Y. Zhang, Z. Fang, C. Fu, and J. Guo, "Effect of pore structures on gas permeability and chloride diffusivity of concrete," *Constr Build Mater*, vol. 163, pp. 402–413, Feb. 2018, doi: 10.1016/J.CONBUILDMAT.2017.12.111.

[5] A. S. Mahmoud, M. M. Yassen, and S. M. Hama, "Effect of glass powder as partial replacement of cement on concrete strength and stress-strain relationship," in *12th International Conference on Developments in eSystems Engineering, (DeSE)*, Kazan: Institute of Electrical and Electronics Engineers Inc., Oct. 2019, pp. 109–114. doi: 10.1109/DESE.2019.00030.

[6] M. Pauletta, N. Rovere, N. Randl, and G. Russo, "Bond-Slip Behavior between Stainless Steel Rebars and Concrete," *Materials* , vol. 13, no. 4, p. 979, Feb. 2020, doi: 10.3390/MA13040979.

[7] C. Rockson, K. Tamanna, M. S. Alam, and A. Rteil, "Effect of cover on bond strength of structural concrete using commercially produced recycled coarse and fine aggregates," *Constr Build Mater*, vol. 255, Sep. 2020, doi: 10.1016/J.CONBUILDMAT.2020.119275.

[8] Z. Zhou and P. Qiao, "Bond behavior of epoxy-coated rebar in ultra-high performance concrete," *Constr Build Mater*, vol. 182, pp. 406–417, Sep. 2018, doi: 10.1016/J.CONBUILDMAT.2018.06.113.

[9] H. S. Ubeid, S. Mahmoud Hama, and A. Shakir Mahmoud, "Mechanical Properties, Energy Impact Capacity and Bond Resistance of concrete incorporating waste glass powder," *IOP Conf Ser Mater Sci Eng*, vol. 745, no. 1, pp. 757–899, Mar. 2020, doi: 10.1088/1757-899X/745/1/012111.

[10] J. Xiao, X. Long, M. Ye, H. Jiang, L. Liu, and K. Zhai, "Experimental Study of Bond Behavior Between Rebar and PVA-Engineered Cementitious Composite (ECC) Using Pull-Out Tests," *Front Mater*, vol. 8, p. 25, Mar. 2021, doi: 10.3389/FMATS.2021.633404.

[11] J. Cai, J. Pan, J. Tan, and X. Li, "Bond behaviours of deformed steel rebars in engineered cementitious composites (ECC) and concrete," *Constr Build Mater*, vol. 252, Aug. 2020, doi: 10.1016/J.CONBUILDMAT.2020.119082.

[12] K. M. A. Hossain, S. Alam, M. S. Anwar, and K. M. Y. Julkarnine, "Bond strength of fibre-reinforced polymer bars in engineered cementitious composites," in *Proceedings of the Institution of Civil Engineers - Construction Materials*, ICE Publishing, Jan. 2020, pp. 15–27. doi: 10.1680/JCOMA.17.00020.

[13] H. Wang, X. Sun, G. Peng, Y. Luo, and Q. Ying, "Experimental study on bond behaviour between BFRP bar and engineered cementitious composite," *Constr Build Mater*, vol. 95, pp. 448–456, Oct. 2015, doi: 10.1016/J.CONBUILDMAT.2015.07.135.

[14] M. Deng, J. Pan, and H. Sun, "Bond behavior of steel bar embedded in Engineered Cementitious Composites under pullout load," *Constr Build Mater*, vol. 168, pp. 705–714, Apr. 2018, doi: 10.1016/J.CONBUILDMAT.2018.02.165.

[15] B. E. Achara, B. S. Mohammed, and M. S. Liew, "Bond behaviour of nano-silica-modified self-compacting engineered cementitious composite using response surface methodology," *Constr Build Mater*, vol. 224, pp. 796–814, Nov. 2019, doi: 10.1016/J.CONBUILDMAT.2019.07.115.

[16] A. H. Alwan Al-Zuhairi and W. Dhaif Sahi Al-Fatlawi, "Numerical Prediction of Bond-Slip Behavior in Simple Pull-Out Concrete Specimens," *Journal of Engineering*, vol. 19, no. 1, pp. 1–12, Jan. 2013, Accessed: Apr. 06, 2023. [Online]. Available: https://www.iasj.net/iasj/download/7e8a3f064bd105b8